Acta Geod Geophys (2015) 50:21–37
DOI 10.1007/s40328-014-0082-4

Seismic hazard and risk assessment based on the unified scaling law for earthquakes

A. Nekrasova · V. G. Kossobokov · I. A. Parvez · X. Tao

Received: 15 September 2014 / Accepted: 3 November 2014 / Published online: 12 December 2014

Abstract The Unified Scaling Law for Earthquakes (USLE), that generalizes the Gutenberg–Richter recurrence relation, has evident implications since any estimate of seismic hazard depends on the size of territory that is used for investigation, averaging, and extrapolation into the future. Therefore, the hazard may differ dramatically when scaled down to the proportion of the area of interest (e.g. a city) from the enveloping area of investigation. In fact, given the observed patterns of distributed seismic activity the results of multi-scale analysis embedded in USLE approach demonstrate that traditional estimations of seismic hazard and risks for cities and urban agglomerations are usually underestimated. Moreover, the USLE approach provides a significant improvement when compared to the results of probabilistic seismic hazard analysis, e.g. the maps resulted from the Global Seismic Hazard Assessment Project (GSHAP). In this paper, we apply the USLE approach to evaluating seismic hazard and risks to population of the three territories of different size representing a sub-continental and two different regional scales of analysis, i.e. the Himalayas and surroundings, Lake Baikal, and Central China regions.

Keywords Seismic hazard · Unified scaling law · Seismic risk · Peak ground acceleration

A. Nekrasova (✉) · V. G. Kossobokov
Institute of Earthquake Prediction Theory and Mathematical Geophysics,
Russian Academy of Sciences, Moscow, Russian Federation
e-mail: nastia@mitp.ru

V. G. Kossobokov
Institut de Physique du Globe de Paris, Paris, France

I. A. Parvez
CSIR Centre for Mathematical Modelling and Computer Simulation, Bangalore, India

X. Tao
Harbin Institute of Technology, Harbin, People's Republic of China

1 Introduction

Losses from natural disasters continue to increase mainly due to poor understanding by majority of scientific community, decision makers and public, the three components of *risk*, i.e. *hazard*, *exposure*, and *vulnerability*. Contemporary science is responsible for not coping with challenging changes of *exposures* and their *vulnerability* inflicted by growing population, its concentration, etc., which result in a steady increase of losses from natural hazards. Scientists owe to society for lack of knowledge, education, and communication. In fact, contemporary science can do a better job in disclosing *natural hazards*, assessing *risks*, and delivering such knowledge in advance catastrophic events.

Our knowledge of *seismic hazard* is rather limited. Sizing earthquakes remains a complicated area of the existing determinations of earthquake magnitudes of different kinds that may reflect an empirical link to energy or moment release, volume, area, or linear extent of rupture, etc. (Bormann 2012). Usually, the accuracy of a magnitude determination depending on the parameters of seismograph records, their networking, and sampling for computations has intrinsic uncertainty of about a factor of two for linear dimensions, i.e. about 0.3 for units of magnitude, due to the observed multiplicative scaling of earthquake sizes. This multiplicative kind of scaling predetermined the choice of the logarithmic scale introduced by Charles F. Richter (Richter 1935) as an instrumental magnitude determination related to earthquake source. Moreover, in 1934 already it was "found that the seismic energy liberated in a given region during a given period is almost wholly accounted for by the larger shocks; the smaller shocks are not sufficiently frequent to contribute more than a small fraction of this energy. It follows that the smaller shocks do not appreciably mitigate the strains which are released in the larger earthquakes, but must be regarded as minor incidents in and symptoms of the accumulation of such strains." Such a scaling is naturally suggestive of a self-similarity of seismic process further investigated later by Gutenberg and Richter (1954) globally, who developed the empirical relationship between the number of earthquakes and their magnitude, now called the Gutenberg–Richter recurrence law. Earthquake recurrence, the one of the larger shocks, in particular, is a critical point of any seismic hazard analysis and assessment of associated risks.

Even nowadays accurate location of earthquake sources depends heavily on the existing networks of seismographs and may vary from a hundred meters or less (e.g. in Japan) to an undefined km (e.g. up to about a hundred km in Southern Pacific). Nevertheless, the accumulated data on hypocenters provides enough evidence for assuming that locally seismic locus generating earthquakes might have a self-similar structure of fractures of different size (e.g., Kossobokov and Mazhkenov 1988; Bak et al. 2002). In such a peculiar geometrical settings, an earthquake recurrence rate at a given site of special concern (e.g., a settlement) would be underestimated if adjusted in proportion to the area from the enveloping region: for example, the underestimation of seismic hazard is a factor of 6.2 for the urban agglomeration of Los Angeles when rescaled from the recurrence rate in the entire area of Southern California (Nekrasova and Kossobokov 2005). Following Bak et al. (2002) the generalization of the Gutenberg–Richter recurrence law accounting for fractal dimensionality of potential seismic sources is denoted as the Unified Scaling Law for Earthquakes, or USLE. In fact, the multi-scale analysis involved in evaluation of the USLE coefficients at a given site combines recurrences for earthquakes obtained from the enveloping areas of different size, so that to get enough statistics on larger magnitude shocks from larger territories around for a reliable confident estimation of scaling.

In this paper we describe the methodology of multi-scale analysis of seismic recurrence along with the algorithm for estimating scaling coefficients of USLE, and then apply it to evaluating seismic hazard and risks to population of the three territories of different size,

i.e. the Himalayas and surroundings (about 18 mln km^2), Lake Baikal (about 2 mln km^2), and Central China (about 1 mln km^2) regions. We conclude with a comparison of the resulting hazard maps based on the USLE against the Global Seismic Hazard Assessment Program Peak Ground Acceleration Map (Giardini et al. 1999), and check both against real earthquakes as reported in the USGS/NEIC Global Hypocenters Data Base.

2 Method

The Gutenberg–Richter recurrence law (Gutenberg and Richter 1954), the most reliable and generally accepted law of similarity in seismology, establishes the relation for a given space-time volume between the annual number of earthquakes, N, and magnitude, M,

$$log_{10}N\,(M) = a - b\,(M - 5)\,,\ \underline{M} \le M \le M*, \tag{1}$$

where $\underline{M}$ and $M*$ are lower and higher magnitude cutoffs. The coefficient a characterizes the expected level of seismic activity in the area, and b reflects changes in the number of earthquakes in successive magnitude ranges. Evidently (1) does not provide any information on the size of the region considered. Following Kossobokov and Mazhkenov (1988, 1994) let us assume that a sequence of earthquakes is self-similar in space, that is, there are no principal differences with respect to the spatial pattern of a set of epicenters, when considered at different scales. The spatial averaging is performed over the areas supporting epicenters of earthquakes from a given magnitude range, so that the areas are not considered if there were no such earthquakes in the period of investigation,.

Let $N(M, L)$ be the expected annual number of earthquakes in a seismic area of linear dimension L. In the case of similarity, the correspondence between $N(M, L)$ and $N(M)$ from the Gutenberg–Richter law can be represented as $N(M, L) = N(M)(L/l)^C$, where $N(M) = N(M, l)$ and l is the characteristic reference length of the region and C is a scaling constant.

Thus, the Gutenberg–Richter recurrence law (1) can be rewritten as

$$log_{10}N\,(M, L) = A + B\,(5 - M) + C log_{10}L \tag{2}$$

The coefficients A and B are similar to a and b from Eq. (1). According to the concept of hierarchy and self-similarity in Earth dynamics, the coefficient C is the fractal dimension (Mandelbrot 1982) of the set of epicenters, which shows how the number of quakes, N, is changing with linear dimension, L, of an enveloping area. The fractal dimension is a notion that can be defined only locally, that is, at a given point of a set. It is the same for all points in case of a homogeneous and self-similar set, i.e. a mono-fractal. It is rather difficult to estimate the fractal dimension of a set using a sample of points, because, first of all, the fractal dimension of any finite (even very large, as well as of any infinite discrete) set equals 0, and, second, the estimate can be biased by the inadequate choice of areas used for a computation.

Usually, in the case where the fractal dimension of a seismic locus at the surface of the Earth is estimated from earthquake catalogs, statistics are representative for areas with a linear size of about tens of kilometers only. A set of possible epicenters is approximated by a finite number of reported events from a catalog where the coordinates are subject to some error. Furthermore, it is obvious that the spatial distribution of earthquakes is not uniform, and it is clear that this distribution is regionally inhomogeneous. Notwithstanding the above mentioned general and earthquake specific difficulties, some practical recipes may be consistent in modeling properties of naturally fractured lithosphere of the Earth, if we accept the hypothesis that the seismic process is self-similar, at least locally, and estimate the coefficients of Eq. (2).

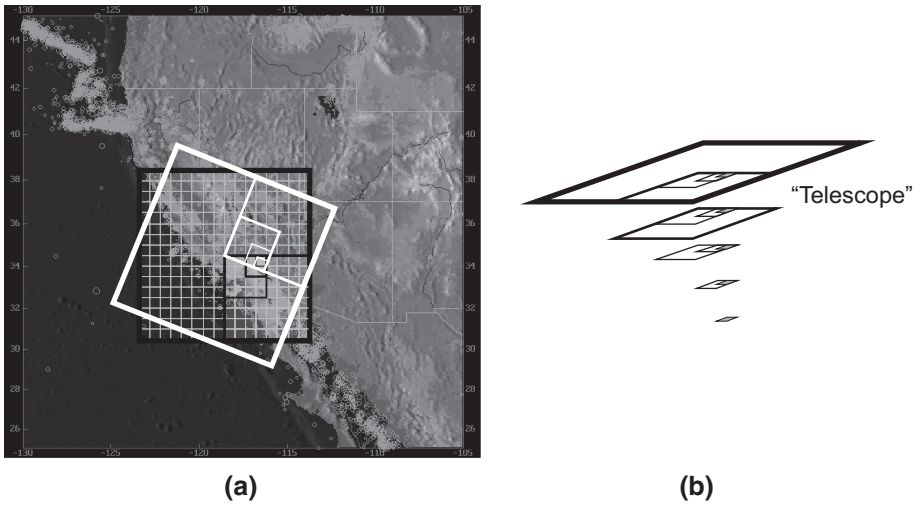

Fig. 1 Illustration of the SCE algorithm: the algorithm is applied 100 times with randomly rotated box counting settings at each grid point on the map; white set of *squares* define an expanding set of *boxes* for the counts of earthquake epicenters (**a**), denoted as "telescope" (**b**)

3 The algorithm

The algorithm of Scaling Coefficients Estimation, SCE (Nekrasova and Kossobokov 2002) is a modified version of its prototype described for the first time in (Kossobokov and Mazhkenov 1988). Let us remind and illustrate the SCE algorithm (Nekrasova et al. 2011).

A catalogue of earthquakes is used as initial input data source. A space-time-magnitude volume, $S \times T \times M$ is considered, where S is the territory, T is time interval from T_0 to T_1, and M is the magnitude range above M_0; the events with magnitude m $\geq M_0$ are reasonably complete in the catalogue since T_0. The input data are processed as follows (Fig. 1):

1. The magnitude range M is subdivided into q adjacent intervals of length ΔM

$$M_j = \{m : M_0 + (j-1)\Delta M \leq m < M_0 + j\Delta M\}, \quad j = l, 2, \ldots, q.$$

2. The entire area S is subdivided into a hierarchy of h levels. The 0-level corresponds to the entire S imbedded in a square of side length L_0. (To avoid double-counting at the borders, a square of side length L here is a set $\{(x, y) : x_1 \leq x < x_1 + L;\ y_1 \leq x < y_1 + L\}$). In the two successive levels i and $i+1$ ($i = 0, l, \ldots, h-1$) of hierarchy each square of side length L_i is split into the four equal squares of side length $L_{i+1} = L_i/2$. A square at the level i of this hierarchy can be denoted as $w_i(e)$ for any point e inside it and, at the same time, as Q_r^i where r is the index number of this square between 1 and 4^i.
3. Using the earthquake catalog, for each one out of the q magnitude ranges and for each one out of the h levels of hierarchy, the following number N_{ji} is computed

$$N_{ji} = \left[\sum \left(n_j\left(Q_r^i\right)\right)^2\right] / N_j \tag{3}$$

where summation extends over all areas $\{Q_r^i\}$ at the i-th level of hierarchy; $n_j(Q_r^i)$ is the number of events from a magnitude range M_j in an area Q_r^i of linear size L_i; N_j is the total number of events from a magnitude range M_j.

Number N_{ji} can be considered as a mean of the number of seismic events in the magnitude range M_j in an area at i-th level of hierarchy, where the mean is calculated over the set of epicenters from M_j. To show this, let us call a telescope a set of the h embedded squares, $W = \{w_0, w_1, \ldots, w_{h-1}\}$, so that each w_i belongs to the i-th level of hierarchy. For a fixed setting of hierarchy, each "telescope" is uniquely defined by w_{h-1} from the smallest size squares. Each of the epicenters of earthquakes, e_k, from the magnitude range M_j catalogue, $E_j = \{e_1, e_2, , , , , e_{Nj}\}$, defines a "telescope" $W(e_k)$ such that $w_{h-1}(e_k)$ contains the epicenter e_k. Consider a set of "telescopes" $\{W(e_k)\}$ defined by the entire set E_j and denote $n_j(w_i)$ as the number of earthquakes from E_j that fall within w_i. Then the mean number of quakes in an area of the i-th level of hierarchy over the entire sample E_j equals

$$N_{ij} = \left[\sum_{k=1}^{Nj} nj\,(w_i(e_k))\right] \Big/ N_j \tag{4}$$

Substituting summation over the events from E_j by summation over the same squares $w_i(e_k) = Q_r^i$ we obtain Eq. (3) implying $N_{ij} = N_{ji}$. Thus, a set of counts $n_j(w_i(e_k))$ provides data for an estimate of fractal dimension of seismic locus at the point e_k and the numbers $N_{ij} = N_{ji}$ are averages of these data. It should be mentioned that this estimate of fractal dimension suggested in (Kossobokov and Mazhkenov 1988, 1994), although originally very close in motivation to estimation of the Hausdorff capacity dimension D_0 (Mandelbrot 1982), in essence, corresponds to the correlation dimension D_2 (Atmanspacher et al. 1988).

Usually, N_{ji} are normalized in time to 1 year and in space to an area of 1 degree of the Earth meridian in length. The graphs of typical counts of N_{ji} for a region are shown in Fig. 2: a model sample of "epicenters" on the classical Koch's curve and the real one for the area of Los-Angeles mega-agglomeration (Figs. 2a, b) are well constrained, while a sample from the US Geological Survey and National Earthquake Information Center, USGS/NEIC, Global Hypocenters Data Base system catalogue (GHDB 1989) for an area of Tokyo (Fig. 2c) may exemplify possible complications and the heuristic adjustments for heterogeneity of seismic distribution of the SCE algorithm.

4. Estimates of A, B, and C in (2) are derived from the set of linear algebraic equations $log_{10}N_{ji} = A - B(M_j - M_0) + ClogL_i$ by the least squares method. Unlike many other recent applications (e.g., Bak et al. 2002) the method makes heuristic adjustments for heterogeneity of seismic distribution, as well as for consistency of the real data statistics in different magnitude ranges. Specifically, the equations that correspond to evidently incomplete samples of data due to extremely low recurrence rates of higher magnitude earthquakes in an area are excluded from computations (Fig. 2c). For this purpose a heuristic limitation requiring $log_{10}(N_{j,i}/N_{j+1,i}) > const$ on transfer from the magnitude range M_j to M_{j+1} (where const is a free parameter of the SCE algorithm, usually set to 2) is used. Similar limitation, $log_{10}(N_{j,i}/N_{j,i-1}) > const$, is introduced for the transfer from $(i-1)-$th to i-th level of spatial hierarchy.
5. In addition to the original prototype algorithm (Kossobokov and Mazhkenov 1988), the steps 1–4 are applied many (usually 100) times with randomized box counting settings at each seismically active location (Nekrasova and Kossobokov 2002). The resulting series of multiple estimates of the three coefficients are used to determine the final average values of A, B, and C along with their standard errors σ_A, σ_B, and σ_C.

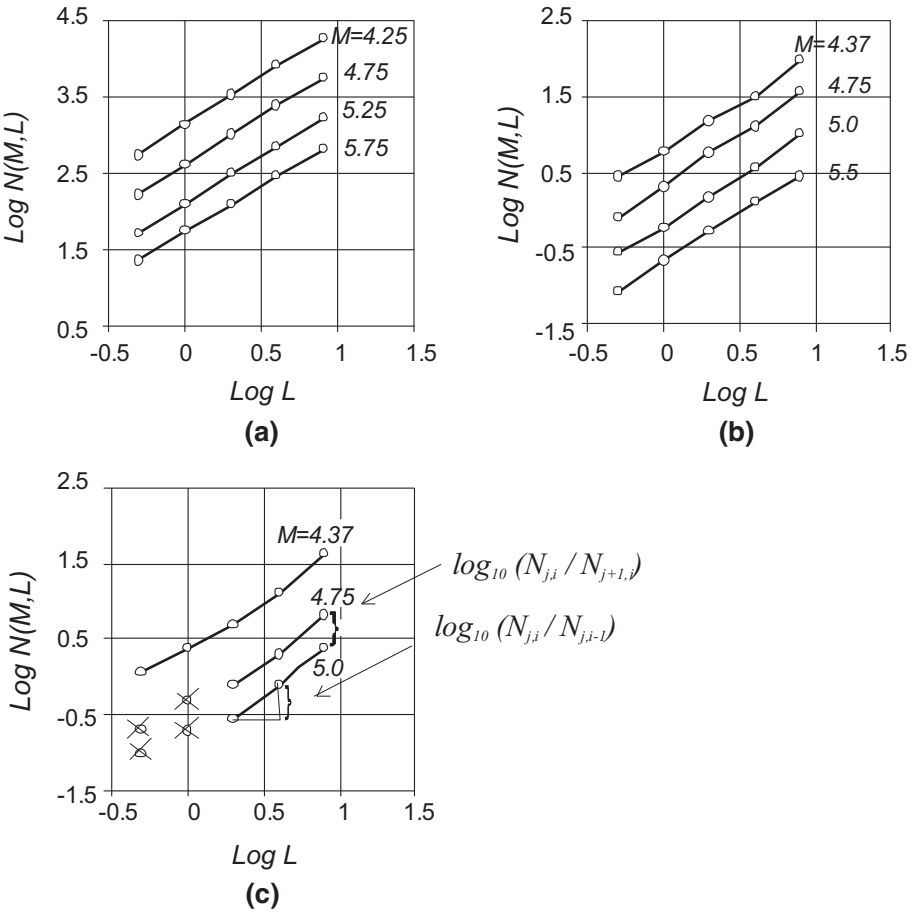

Fig. 2 A typical sets N_{ji} counts for a region: **a** a model sample of epicenters on the Koch's curve, **b** epicenters at Los-Angeles region, and **c** epicenters near Tokyo agglomeration

4 Direct implications for seismic hazard and risk estimates

Any kind of risk estimates results from a convolution of the hazard with the exposed object under consideration along with its vulnerability

$$R(g) = H(g) \otimes O(g) \otimes V(O(g)),$$

where $H(g)$ is natural hazard at location g, $O(g)$ is the exposure of objects at risk at g, and $V(O)$ is the vulnerability of objects at risk. Note that g could be a point, or a line, or some area on or under the Earth surface and that distribution of hazards, as well as objects of concern and their vulnerability, could be time-dependent. Furthermore, the convolution $\otimes$ could be much more complicated operation than usually accepted product of terms.

In the case of seismic phenomenon the key role in the risk assessment is related to the choice of a probability model describing the occurrence of earthquakes in a specified space-magnitude-time volume $V = \{g, M, t\}$. A rough description of the leading features for long-term seismic activity is usually provided by assuming the flow of events $(g, M, t) \in V$

to be a stationary point Poisson process with annual rate of $N(M)$, which according to the well-established Gutenberg–Richter law (1) is parameterized in a log-linear form (Molchan et al. 1997). Seismic reality evidences many contradictions to this assumption that have led to complications of the existing hypotheses by introducing de-clustered sequences of main events and their associates (fore- and after-shocks) superimposed with hypothetical distributions of the associate size, time, and location. In any case, the estimation of $N(M)$ at a given site of interest remains the basic source of seismic risk assessment, as well as the basic source of inadequate seismic engineering decisions.

By applying USLE that generalizes the Gutenberg–Richter recurrence relation to evident patterns of distributed seismic activity one can demonstrate that the traditional estimations of seismic risk for cities and urban agglomerations are usually underestimated. In fact, any estimate of seismic hazard rate (e.g., $N(M)$) depends on the size of territory that is used for averaging and, therefore, may differ dramatically when scaled down to the proportion of the area of interest. For example, the coefficient C at Los Angeles is about 1.21 both as estimated by Okubo and Aki (1987) for the system of faults in Southern California and as computed by applying the SCE algorithm to one of the best regional earthquake catalogues; scaling down in proportion to the area from the entire Southern California of about 400 km to the region of Los Angeles about 40 km in length underestimates the recurrence rate by a factor of $(L_{SCA}/L_{LA})^2/(L_{SCA}/L_{LA})^{1.21} = 10^{0.79} = 6.2$. By analogy, the underestimation seismic hazard in a region of about 40 km long at Petropavlovsk-Kamchatsky from the area of Kamchatka about 700 km in length where C = 1.26 rises to a factor $(L_K/L_{PK})^2/(L_K/L_{PK})^{1.26} = 17.5^{0.74} = 8.3$. A comprehensive analysis of seismic hazard at 1140 cities and urban agglomerations in seismic regions worldwide due to scaling in proportion to the area (Nekrasova and Kossobokov 2005) reveals in addition to abovementioned cases potential underestimation of a factor of 5.4 for Tokyo (Japan), 7.2 for San Francisco (USA), about 20 for Ulan-Ude (Republic of Buryatia, Russian Federation), etc.

Such a discrepancy in evaluation of seismic hazard propagates non-linearly into erroneous estimations of risks. An error in rate of a factor of 6 (in assumption of $B = 1$) corresponds to an error about 0.8 in magnitude, which explodes exponentially in underestimation of seismic energy release by a factor 15 corresponding to a factor above 4.5 for expected fatalities, etc. (Wyss et al. 2012).

5 Mapping seismic hazard based on the USLE approach

In this section we apply the SCE algorithm for compiling the maps of the USLE coefficients for the three territories in Asia of different size representing a sub-continental and two different regional scales of analysis (Fig. 3), i.e. the Himalayas and surroundings, Lake Baikal, and Central China regions. Then the results are used for mapping seismic hazard and risk associated with population.

6 Data

The territory of Himalayas and surroundings is considered within 5°–40°N and 60°– 105°E. The coefficients of USLE are evaluated by applying the SCE algorithm to the sample of about 5,000 earthquakes from the USGS/NEIC Global Hypocenters Database System, 1965–2011 with depth shallower than 100 km (GHDB 1989). The calculations performed using the hierarchy of square cells with linear size of 8°, 4°, 2°, 1°, and 1/2°.

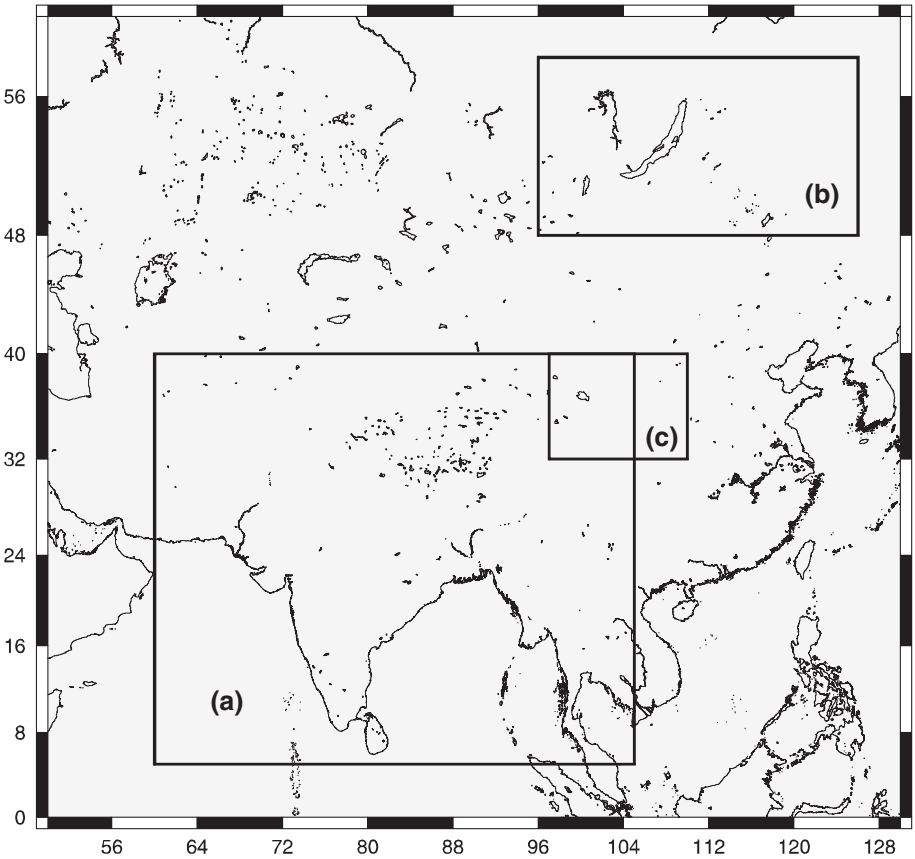

Fig. 3 The three regions: the Himalayas and surroundings (**a**), Lake Baikal (**b**), and Central China (**c**)

Seismicity of Lake Baikal region is considered within 48°–58°N and 96°–126°E. The regional catalog is compiled using the annual periodical "Earthquakes in USSR" and its continuation "Earthquakes in Northeastern" Asia and "Earthquakes in Russia" (through 2008 except for 1992 and 1993) expanded for another 6° to the East from 120°E to 126°E. The regional catalog is sufficiently complete in reporting earthquakes of *energy class* K = 9 or above, which range corresponds to magnitude M = 2.78 or larger. (The energy class determinations were officially adopted and widely used in the Soviet Union.) The SCE algorithm was applied to the sample of all 10546 earthquakes with depth above 100 km and the hierarchy of square boxes with linear size of 8°, 4°, 2°, 1°, and 1/2°.

The territory within 32–40°N and 97–110°E in Central China represents the smallest region of the three considered here. For application of the SCE algorithm we used the sample of 2044 normal depth seismic events with magnitude 4.0 or more reported in China Earthquake National Catalog (CENC 2014), 01/01/1970–01/07/2013, and the hierarchy of areas with linear size of 4°, 2°, 1°, 1/2°, and 1/4°.

For each of the three regions Fig. 4 presents the empirical density distribution ρ determined by the sample of seismic events from the USGS/NEIC Global Hypocenters Database System, 1965–2011. Note that the density total in a region equals to 1, and each cell on a map is shade-of-grey-coded according to the logarithm of its empirical density function value. The three

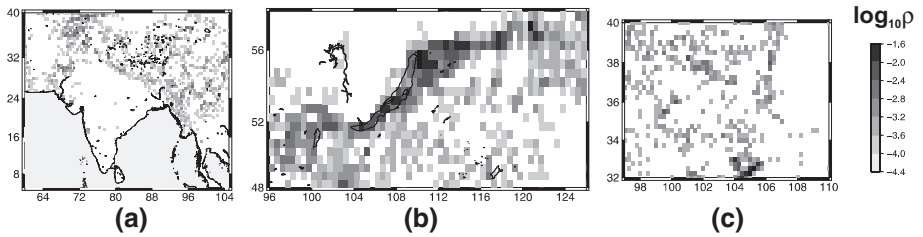

Fig. 4 The maps of the logarithm of the empirical density distribution function of seismic activity: the Himalayas and surroundings (**a**), Lake Baikal (**b**), and Central China (**c**)

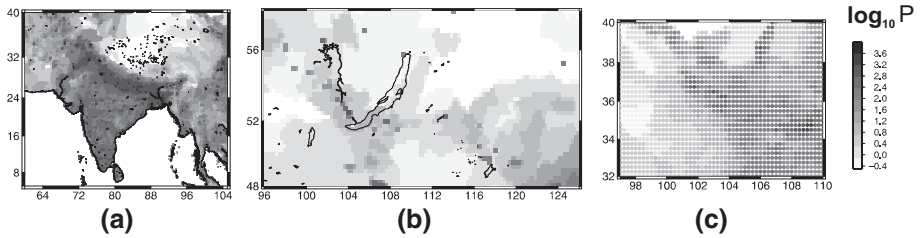

Fig. 5 The logarithm of the population density (based on GPWv3 estimate for 2010): the Himalayas and surroundings (**a**), Lake Baikal (**b**), and Central China (**c**)

maps are, in a sense, the best knowledge of where earthquakes did and may happen in the future, and, therefore, determine seismically active locations for the SCE algorithm box counting settings.

In addition to seismic data and for the purposes of a model risk assessment, we consider the population density maps for the three territories. The data on population are taken from Gridded Population of the World (GPW 2005), GPWv3, that is a raster data product compiled at Center for International Earth Science Information Network (CIESIN), Columbia University, and Centro Internacional de Agricultura Tropical (CIAT). It renders global population data at the scale and extent, required for demonstrating the spatial relationship of human populations and the environment across the globe. The database provides a spatially disaggregated population layer that is compatible with data sets from social, economic, and Earth science fields. We have chosen the estimates of population density for the year 2010 (Fig. 5) to assess a model risk associated with seismic hazard.

7 Results

The results of the SCE algorithm application are given in Fig. 6. Each of the upper first three rows displays of the three maps of the USLE coefficient (A in the 1st, B–2nd, and C– 3rd row, respectively). The bottom row demonstrates the three regional probability density distributions of the estimated values for each of the three USLE coefficients: Coefficient A represents logarithm of seismic activity, B characterizes the balance between magnitude ranges, and C corresponds to the estimate of the fractal dimension of seismic locus at a given location.

The range of seismic activity in the three regions is rather different: the annual rate of magnitude 5 quakes in a $1^\circ \times 1^\circ$ square (i.e. 10^A) is mainly between 0.2 and 1.3 in Himalayas and surroundings, between 0.003 and 0.02 in Lake Baikal, and between 0.07 and 0.6 in Central China region. In the three regions the magnitude balance B, analogous to b-value

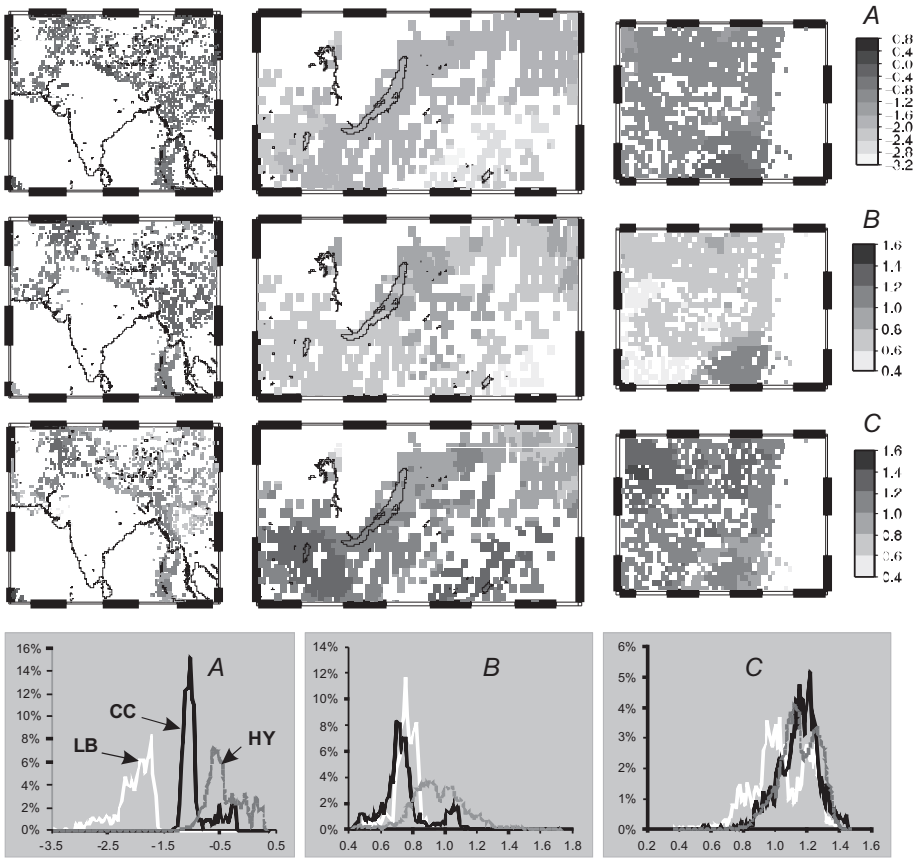

Fig. 6 The regional maps of A, B, and C coefficients (*upper three rows*) and their empirical probability density distribution functions (*bottom row*) for Himalayas and surroundings (HY), Lake Baikal (LB), and Central China (CC)

in the Gutenberg–Richter relation, spreads mainly within 0.8–1.2, 0.7–0.8, and 0.6–1.0, respectively. The empirical probability density of the fractal dimension of seismic loci C in Himalayas and surroundings and Central China region are rather similar in shape ranging from about 1 to 1.3, while the one for Lake Baikal has three separate peaks at 0.8, 1.0, and 1.2, the values about which are attributed to the vast territories with different level of tectonic fracturing (e.g., western Stanovoy Ridge, Baikal Rift, and Sayan Mountains, correspondingly; the minimal values of the fractal dimension C are found for the Bratsk Reservoir area may be related to induced seismicity). It should be noted that the results for the Lake Baikal region are in full agreement with our previous analysis based on data to 1997 (Nekrasova and Kossobokov 2006) and, naturally, provide an improvement being supported with an additional decade of data.

The USLE coefficients were used for estimation and mapping the expected maximum magnitude M_{max} with a 10 % chance of exceedence in 50 years following the procedures suggested in (Parvez et al. 2014). Specifically, for each $0.5^\circ \times 0.5^\circ$ cell at seismic location on a regional map (Figs. 4, 6) we apply formula (2) to calculate the expected numbers of events from magnitude ranges M_j in 50 years, i.e. $N_{50}(M_j, 0.5^\circ) = 50 \times N(M_j, 0.5^\circ)$, and then find

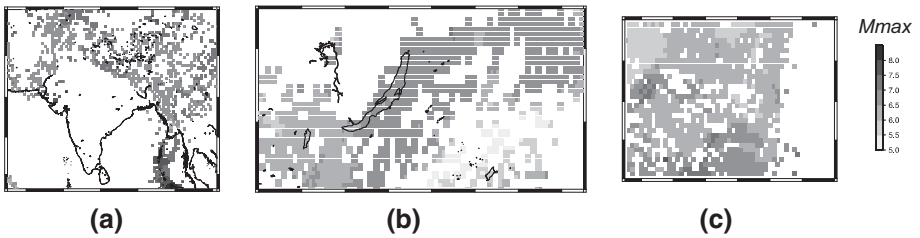

Fig. 7 The seismic hazard maps for the three regions in terms of M_{max}: the Himalayas and surroundings (**a**), Lake Baikal (**b**), and Central China (**c**)

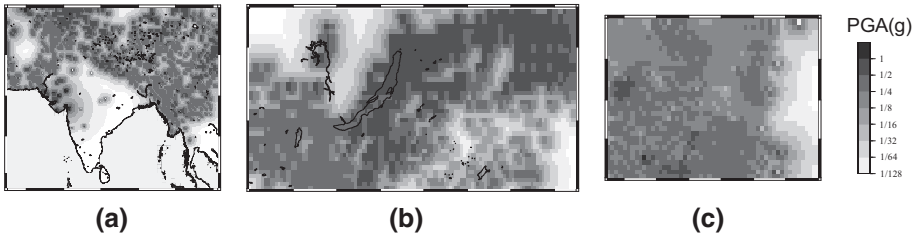

Fig. 8 The three seismic hazard maps in terms of PGA (in g) based on USLE approach: the Himalayas and surroundings (**a**), Lake Baikal (**b**), and Central China (**c**)

the maximum magnitude, $M_{\max}$, with the expected number $N_{50}(M_{\max}, 0.5°) \geq 10\,\%$. Figure 7 shows the three regional maps of the $M_{\max}$ values assigned in such a way. Naturally, these are the estimates of traditional maximum magnitude with 10 % chance of exceedence in 50 years.

These maps were used to estimate the hazard maps in terms of expected ground shaking measured by Peak Ground Acceleration, PGA. The semi-empirical relations linking the interdependence among the peak ground motion, earthquake magnitude and distance to hypocenter for the regions under investigation were determined by Parvez et al. (2001) from strong motion data available. Figure 8 shows the three regional seismic hazard maps in terms of PGA determined as follows. For each grid point we apply the empirical formula (5) for acceleration produced by a source of $M_{\max}$ as inspired from (Parvez et al. 2001)

$$\mathrm{Acc}(M_{\max}, D) = \mathrm{const} \times \mathrm{g} \times D^{-1.5} \times exp(M_{\max} - 5), \tag{5}$$

where D is the source-receiver distance on a $0.25° \times 0.25°$ grid, const = 6, $g = 9.81$ m/s^2 is the gravity constant, and $exp(x)$ is the natural exponent of x. The maximum of acceleration values computed at a grid point is assigned to it. We have opted the minimum and maximum distances of 10 and 500 km, respectively.

8 Comparison and verification of the results

The Global Seismic Hazard Assessment Program (GSHAP) was initiated in 1992 and approved as a demonstration project under the International Decade for Natural Disaster Reduction declared by the United Nations Organization (UN/IDNDR). The GSHAP was completed in 1999 and the probabilistic seismic hazard assessment maps (Giardini et al. 1999; Shedlock et al. 2000) displaying global distribution of maximum PGA with 10 % chance of exceedence in 50 years in the $0.1° \times 0.1°$ mesh were published (the archive containing the GSHAP PGA numerical evaluations for the whole world is in open access at

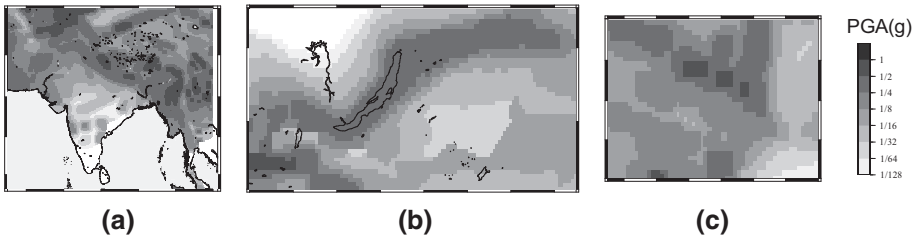

Fig. 9 The three maps of PGA (in g) as given on the final GSHAP seismic hazard map: the Himalayas and surroundings (**a**), Lake Baikal (**b**), and Central China (**c**)

http://www.seismo2009.ethz.ch/GSHAP/gshpub.zip). After the 2010 Haiti disastrous earthquake and a number of other failures of GSHAP maps we performed a systematic study (Kossobokov and Nekrasova 2010) coming to conclusion that Global Seismic Hazard Assessment Program Maps are misleading. After the 2011 Tohoku mega-thrust the conclusion was confirmed (Kossobokov and Nekrasova 2012) and further highlighted the importance of testing the model maps with observations (Albarello and D'Amico 2008; Wasserburg 2010; Stein et al. 2012). Although the GSHAP maps cannot be further used for a responsible assessment of seismic risks, we use it (Nekrasova et al. 2014a, b) for the purposes of comparison with other SHA maps available including its most recent versions prepared in the frames of Seismic Hazard Harmonization in Europe (Giardini et al. 2014) and ground shaking maps based on the physically and mathematically rooted neo-deterministic approach (Panza 2013).

Figure 9 shows the GSHAP PGA maps of the three regions. Evidently, the maps obtained by GSHAP differ from those based on USLE in Fig. 8 dramatically. At a glance the USLE based maps appear to be more selective and avoid some of the errors of GSHAP like the locations of the 2001 Bhuj and 2004 Sumatra-Andoman great earthquakes on the sub-continental scale map of Himalayas and surroundings.

Let us check both approaches at the locations of real earthquakes of magnitude 5 or larger with hypocenters above 70 km as reported in the Global Hypocenters Data Base System (GHDB 1989) for the time period from 1900 to the present. Table 1 lists the number of earthquakes with the estimated PGA values at epicenter exceeding the value on the model map by a factor of 2, or 4, or 8, which factor corresponds to the level of acceptability of an error and, roughly, to underestimation by 1, 2, and 3 units of macroseismic intensity. These numbers are counted for the three magnitude ranges of moderate, strong, and significant earthquakes ($M \geq 5.0$, $M \geq 6.0$, and $M \geq 7.0$, respectively).

As evident from Table 1 the USLE model outscore GSHAP in identifying correctly the sites of moderate, strong, and significant earthquakes. Specifically, the number of unacceptable errors, when PGA value on a map at epicenter of real earthquake is by factor 2 or greater less than attributed to this earthquake, is several times larger for the GSHAP map than for the USLE one (e.g., 11.4, 1.7, and 2.5 times for strong earthquakes in Himalayas and surroundings, Lake Baikal, and Central China region, respectively). This cannot be attributed to the difference of the empirical probability distributions of the model PGA values in a region, although evidently USLE model favors larger estimates in Baikal and Central China regions (Fig. 10). Note that at the regional scale of investigation the GSHAP estimates of seismic hazard can be grossly underestimated in the areas of sparse explorations of seismically active faults, like those to the east of the upper segment of the Baikal rift zone.

For both models the percentage of unacceptable errors increase with magnitude: from 2 to 27 % for GSHAP and from 1 to 4 % for USLE in Himalayas, from 4 to 43 % for GSHAP

Table 1 The number of earthquakes with the estimated PGA values at epicenter exceeding the value on the model map

Model map	GSHAP				USLE based			
Himalayas and surroundings								
PGA ratio	any	>2	>4	>8	any	>2	>4	>8
M ≥ 5	4,666	86	39	17	4,746	36	23	18
M ≥ 6	702	57	21	8	706	5	2	0
≥ 7	121	33	14	5	121	5	2	0
Lake Baikal region								
PGA ratio	any	>2	>4	>8	any	>2	>4	>8
M ≥ 5	176	7	3	0	176	4	1	1
≥ 6	42	5	3	0	42	3	1	1
M ≥ 7	7	3	2	0	7	2	0	0
Central China region								
PGA ratio	any	>2	>4	>8	any	>2	>4	>8
M ≥ 5	158	5	4	1	158	2	1	0
M ≥ 6	37	5	4	1	37	2	1	0
M ≥ 7	7	4	4	1	7	2	1	0

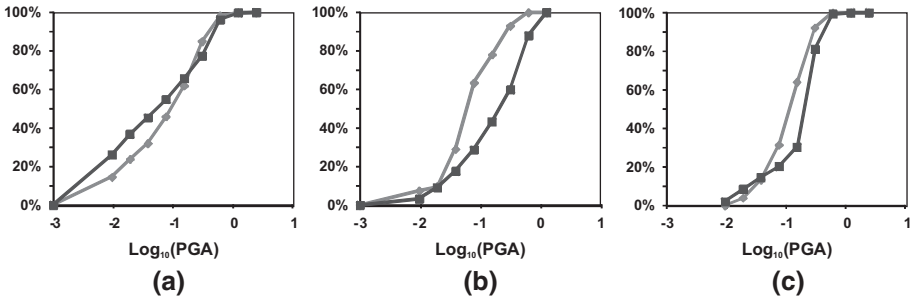

Fig. 10 The empirical probability distributions of the GSHAP (*the line with diamonds*) and USLE (*the line with squares*) PGA values in a region: the Himalayas and surroundings (**a**), Lake Baikal (**b**), and Central China (**c**). *Note* PGA values are in m/s^2; series symbols are at g, g/2, g/2^2, g/2^3, g/2^4, g/2^5, g/2^6, and g/2^7

and from 2 to 29 % for USLE in Baikal, and from 3 to 57 % for GSHAP and from 1 to 29 % for USLE in Central China. It should be noted that on a regional scale these errors are mainly due to a few cases of significant earthquakes, e.g., in Central China region the only two unacceptable errors of the USLE are due to the 16 December 1920, M8.5 Haiyuan and 22 May 1927, M8.0 Gulang great earthquakes, which rather uncertain epicenter determinations are reported in (GHDB 1989). On the other hand we cannot rule out the case of insufficient data available for some territories at the regional scale about 1 mln km^2.

9 Estimation of seismic risks in the three regions

Naturally, there exist many different risk estimates even if the same object of risk and the same hazard are involved. The variety may result from the different laws of convolution, as well as

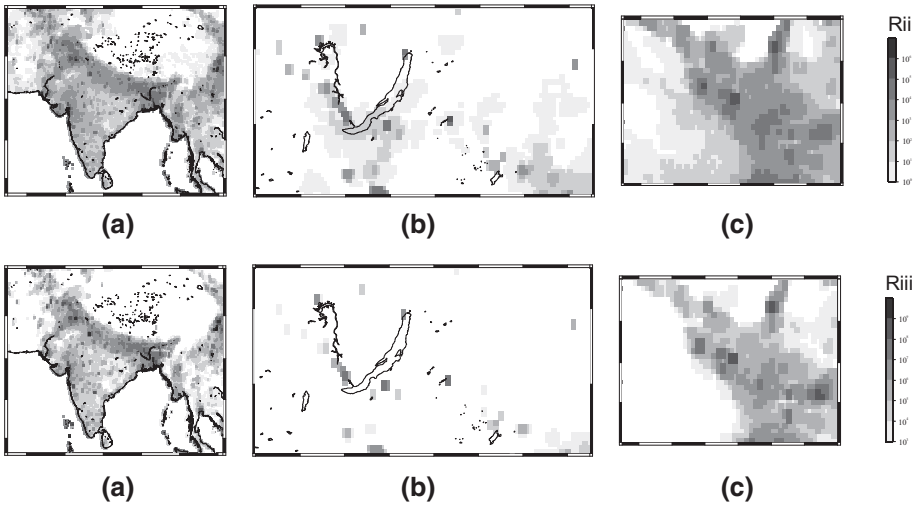

Fig. 11 The maps of seismic risk for population of the three regions: the Himalayas and surroundings (**a**), Lake Baikal (**b**), and Central China (**c**). Oversimplified convolutions of seismic hazard map H(g) with the population density distribution P : $R_{ii}(g) = H(g) \cdot \int_g P \cdot P$ (upper row) and $R_{iii}(g) = H(g) \cdot \int_g P \cdot P^2$ (*bottom row*)

from different kinds of vulnerability of an object of risk under specific environments and conditions. Both the conceptual issues must be resolved in a multidisciplinary problem-oriented research performed by specialists in the fields of hazard, objects of risk, and object vulnerability. To illustrate the concept, we perform the two oversimplified convolutions of seismic hazard assessment map H(g) based on USLE with the population density P suggested in (Parvez et al. 2014). Both risk computations consider the GPWv3 model population data estimates of the year 2010 as an object of risk and use mathematical product as the convolution law.

The first estimate in a cell g is based on the individual vulnerability in proportion to the population density at a given site, $R_{ii}(g) = H(g) \cdot \int_g P \cdot P$, where $\int_g P$ is the integral of the population density over the cell g, i.e. the number of individuals within the area of the cell g. The second risk estimate is $R_{iii}(g) = H(g) \cdot \int_g P \cdot P^2$. Both appear to be rather natural due to specifics of man-made environment inflicted in the areas of high concentration of individuals: the number of floors in typical residential building changes non-linearly with population density. The resulting maps of the two risks in arbitrary units are given in Fig. 11. For illustration purposes, each of the two risk scales is covering the top seven decimal orders of the risk values in the three regions considered, so that the cells in black are 1,000,000 times more dangerous than those in lightest shade of grey. The collapse of the risky areas to the region of the densest population appears rather natural demonstrating how non-linearity of conditions changes expectation of seismic risk. It is notable that, as expected, the mega-cities and their agglomerations are at the top of risk distributions. One can clearly observe that the risks in the areas next to the India-Eurasia continental collision zone (i.e. Himalayas and surroundings as far as to Central China region) are much higher than on its peripheries (e.g., in Baikal region).

To avoid misleading interpretations, we have to emphasize that *the risk estimates presented for the three regions under study are given for academic methodological purposes only*. They do not use complicated procedures that might be more adequate convolutions of hazard, objects of risks, and their vulnerability, and are used here to highlight the general problem-oriented approach. The estimations addressing more realistic and practical kinds of seismic risks should involve experts in earthquake engineering, social sciences and economics.

10 Discussion and conclusion

Earthquakes are not predictable with precision of a certain date and rupture zone. On the other hand, the seismic loci are well exposed due to rather long earthquake history and geologic studies in a few regions and instrumental monitoring of the entire Earth. Strong disastrous earthquakes are low probability events that happen with certainty (i.e. 100 % probability). Since data are insufficient to constrain the probability models, ground shaking probabilities turn out highly uncertain and unreliable, particularly for the large, sporadic and most destructive earthquakes. Low probability earthquake information provided by any group as the basis for probabilistic seismic hazard assessment leads to false comfort of ignoring such rare eventualities, so that they will happen again and again as unexpected disastrous surprises. Comparison of observed numbers of fatalities with those calculated based on expected ground shaking from GSHAP maps (Kossobokov and Nekrasova 2012; Wyss et al. 2012), show that seismic hazard maps based on the standards of probabilistic methodology do not allow to reliably estimate risks to which the population is exposed due to large earthquakes in many regions worldwide.

The largest expected earthquake size for earthquake-prone locations can be realistically estimated with high confidence. Preparing for such hazardous event ensures reduction or even avoidance of potential disasters. Earthquakes do not kill people but their consequences, i.e., tsunamis, land-slides, collapsed buildings, bridges and other constructions, do. The hazard scenarios for such an event estimated by deterministic computations provide the basis for necessary preparations, from land-use planning and building code regulation to emergency management. There are many risks generated by earthquakes. These should be not ignored in any realistic and responsible seismic risk evaluation and knowledgeable disaster prevention.

Our study attempts to contribute modestly to an urgent necessary revision of the seismic hazard maps from the first principles, including (i) background methodologies and (ii) implementation in assessment of seismic risks. Evidently, our contribution at this time (i) takes into consideration economic and social factors of risk assessment in an oversimplified way of pilot studies, (ii) does not account for the role of site effect due to topography and soils in determining ground acceleration, and (iii) makes use of a point approximation of an earthquake rupture even for the great and complex seismic events. These essential considerations should be addressed in the future. However, the results of comparison with real seismic activity in the three regions of different size presented in this study permit us to conclude that the USLE approach provides a significant improvement when compared to the results of probabilistic seismic hazard analysis. In fact, hazard assessment based on USLE allows for multi-scale analysis of seismic recurrence at a given earthquake prone site, which combines statistics obtained from the enveloping areas of different size, so that to get enough larger magnitude shocks from larger territories around for a reliable confident estimation of scaling and the largest expected earthquake size.

Acknowledgments The authors acknowledge the support from the Russian Foundation for Basic Research, Department of Science and Technology of India, and GFNS of People's Republic of China (Grants RFBR 1 13-05-91167, GFNS No. 51311120080, RFBR 1 14-05-92691, and DST No. INT/RFBR/P-176).

References

Albarello D, D'Amico V (2008) Testing probabilistic seismic hazard estimates by comparison with observations: an example in Italy. Geophys J Int 175:1088–1094

Atmanspacher H, Scheingraber H, Voges W (1988) Global scaling properties of a chaotic attractor reconstructed from experimental data. Phys Rev A 37(4):1314–1322

Bak P, Christensen K, Danon L, Scanlon T (2002) Unified Scaling Law for Earthquakes. Phys Rev Lett 88:178501–178504

Bormann P (Ed) (2012) New manual of seismological observatory practice (NMSOP-2). IASPEI, GFZ German Research Centre for Geosciences, Potsdam; http://nmsop.gfz-potsdam.de; doi:10.2312/GFZ.NMSOP-2urn:nbn:de:kobv:b103-NMSOP-2

CENC (2014) China Earthquake Networks Center Catalog. http://www.csndmc.ac.cn/wdc4seis@bj/intro/cenc/intro.jsp

GHDB (1989) Global Hypocenters Data Base CD-ROM. NEIC/USGS, Denver, CO, 1989 and updates July 2014

Giardini D, Grünthal K, Shedlock P, Zhang (1999) The GSHAP global seismic hazard map. Ann Geofis 42(6):1225–1228

Giardini D, Wössner J, Danciu L (2014) Mapping Europe's seismic hazard. Eos Trans AGU 95(29):261–262

GPW (2005) Gridded Population of the World, Palisades, NY: Socioeconomic Data and Applications Center (SEDAC), Columbia University. http://sedac.ciesin.columbia.edu/gpw. Accessed 29 May 2012

Gutenberg B, Richter CF (1954) Seismicity of the Earth, 2nd edn. Princeton University Press, Princeton 310 p

Kossobokov VG, Mazhkenov SA (1988) Spatial characteristics of similarity for earthquake sequences: Fractality of seismicity. Lecture Notes of the Workshop on Global Geophysical Informatics with Applications to Research in Earthquake Prediction and Reduction of Seismic Risk (15 Nov–16 Dec 1988), ICTP, Trieste

Kossobokov VG, Mazhkenov SA (1994) On similarity in the spatial distribution of seismicity. In: Chowdhury DK (ed) Computational Seismology and Geodynamics/AGU, 1. The Union, Washington, pp 6–15

Kossobokov V, Nekrasova A (2010) Global seismic hazard assessment program maps are misleading. Eos Trans AGU 91(52):U13A–0020

Kossobokov V, Nekrasova A (2012) Global seismic hazard assessment program maps are erroneous. Seism Instrum 48(2):162–170. doi:10.3103/S0747923912020065

Mandelbrot B (1982) The fractal geometry of nature. Freeman, New York

Molchan G, Kronrod T, Panza GF (1997) Multi-scale seismicity model for seismic risk. Bull Seismol Soc Am 87:1220–1229

Nekrasova A, Kossobokov V (2002) Generalizing the Gutenberg–Richter scaling law. EOS Trans AGU 83(47):NG62B–0958

Nekrasova A, Kossobokov V (2005) Unified Scaling Law for Earthquakes: mega-cities and urban agglomerations. Eos Trans AGU 86(52):S23A–0229

Nekrasova A, Kossobokov V (2006) Unified scaling law for earthquakes in the Lake Baikal region. Doklady Earth Sci 407A(3):484–485

Nekrasova A, Kossobokov V, Aoudia A, Perezan A, Panza GF (2011) A multiscale application of the Unified Scaling Law for Earthquakes in the Central Mediterranean area and Alpine region. Pure Appl Geophys 168:297–327

Nekrasova A, Kossobokov V, Peresan A, Magrin A (2014) The comparison of the NDSHA, PSHA seismic hazard maps and real seismicity for the Italian territory. Natl Hazards 70(1):629–641. doi:10.1007/s11069-013-0832

Nekrasova A, Peresan A, Kossobokov VG, Panza GF (2014) A new probabilistic shift away from seismic hazard reality in Italy? Proceedings of the International School and Workshop on "Nonlinear Mathematical Physics and Natural Hazards"; arXiv:1409.1047v2 [physics.geo-ph]

Okubo PG, Aki K (1987) Fractal geometry in the San Andreas fault system. J Geophys Res 92:345–355

Panza GF, Peresan A, La Mura C (2013) Seismic hazard and strong ground motion: an operational neo-deterministic approach from national to local scale. In: UNESCO-EOLSS Joint Committee (Eds) Encyclopedia of life support systems (EOLSS), Geophysics and Geochemistry, Developed under the Auspices of the UNESCO, Eolss Publishers, Oxford, UK, pp 1–49

Parvez IA, Gusev A, Panza GF, Petukhin A (2001) Preliminary determination of the interdependence among strong motion amplitude, earthquake magnitude and hypocentral distance for the Himalayan region. Geophys J Int 144:577–596

Parvez IA, Nekrasova A, Kossobokov V (2014) Estimation of seismic hazard and risks for the Himalayas and surrounding regions based on Unified Scaling Law for Earthquakes. Natl Hazards 71(1):549–562. doi:10.1007/s11069-013-0926-1

Richter CF (1935) An instrumental earthquake magnitude scale. Bull Seismol Soc Am 25(1):1–32

Shedlock K, Giardini D, Grünthal G, Zhang P (2000) The GSHAP global seismic hazard map. Seismol Res Lett 71(6):679–686

Stein S, Geller R, Liu M (2012) Why earthquake hazard maps often fail and what to do about it? Tectonophysics 562(563):1–25

Wasserburg GJ (2010) Comment on "AGU statement: Investigation of Scientists and Officials in L'Aquila, Italy, is unfounded. Eos Trans AGU 91(42):384

Wyss M, Nekrasova A, Kossobokov V (2012) Errors in expected human losses due to incorrect seismic hazard estimates. Natl Hazards 62(3):927–935. doi:10.1007/s11069-012-0125-5